PROCEEDINGS A

rspa.royalsocietypublishing.org

Research

Check for updates

Article submitted to journal

Subject Areas:
Climate Sensitivity

Keywords:
Climate Sensitivity, Local Climate Sensitivity, Impulse Response, sensitivity, ARX method

Author for correspondence:
johnsinclairreid@gmail.com

Statistical Modelling of Climate Time Series

John Reid

New Norfolk, Tasmania, Australia. 7140

Two powerful statistics can be derived from simultaneous time series observations, the impulse response and the sensitivity. The former is the response to a unit impulse in the independent variable and the latter is the response to a unit step function and is the sum of terms of the impulse response sequence. Both statistics can be estimated by means of the ARX method further strengthened by testing residuals for self-correlation. In this way, global climate sensitivity, the long-term increase in global average temperatures due to a doubling of CO2 concentration, was estimated to be 2.7 deg C with 95 percent confidence limits of 2.3 and 3.4. The impulse response of CO2 concentration to a variation in CO2 emissions, was found to be exponential with a half-time of 43 years. The widely accepted hypothesis, that a significant fraction of carbon emissions remain in the atmosphere indefinitely, can be rejected. The method was also applied to local climate sensitivity which varies widely, continental values being generally larger than maritime values.

THE ROYAL SOCIETY
PUBLISHING

1. Introduction

A climate model or coupled ocean-atmosphere general circulation model (OAGCM) is a numerical model of the global atmosphere and ocean based on the Navier-Stokes equations of fluid dynamics. Numerical modelling of an estuary, lake or tidal shelf can be difficult at the best of times but modellers made a quantum leap from such relatively simple exercises into the complex dynamics of an entire planet. They started with the assumption that we already know, *a priori*, the underlying physics and that understanding climate is simply a matter of refining the detail.

OAGCMs cannot account for "unlooked-for combinations of things" which were not considered at the time of setting up the model. An example is the effect of the plume from recent Australian wild fires on fertilization and CO_2 uptake over vast areas of the Pacific and Southern Oceans [1]. Such unforeseen events are beyond the scope of a OAGCMs which resemble the *a priori* celestial models of Ptolomaic astronomy.

The present statistical method makes no assumptions about the underlying physics, other than that the system under investigation is random rather than deterministic and that it is stationary and ergodic.

It is common practice across a wide range of sciences to treat physical quantities as ensemble parameters and to estimate them from sample statistics. A time series is a particularly type of sample, one in which a series of measurements are taken at equal intervals of time or averaged over equal intervals of time. The Pearson correlation coefficient is often used to describe the relationship between contemporaneous time series, but it is a poor statistic because it does not account for temporal ordering. Two other statistics, which better summarize the relationship between two concurrent time series, are the impulse response and the sensitivity. The impulse response is the response of the endogenous or dependant variable to a short pulse in the exogenous or independent variable. The sensitivity may be defined as the response of the endogenous variable to a step-function in the exogenous variable. It is the sum of terms (or integral) of the impulse response.

Both statistics can be estimated using the "autoregressive with exogenous variable" or ARX method. Their existence and the number of ARX regression coefficients required for their computation, is established by rejecting those configurations whose residuals show significant self-correlation. The impulse response is then found as the convolutional reciprocal of a sequence derived from the ARX regression coefficients. These ideas originated with [2] and were recently applied to climate sensitivity by [3]. Here we derive these statistics using convolutional methods and apply them to climate time series.

2. Using the ARX Method

For notational convenience, in the following, all sample means have been removed and random variables are assumed to have zero mean.

The autoregressive moving average method with a single exogenous variable, ARMAX(p,q), is given at time, i, by:

$$Y_i = \alpha_0 x_i + \sum_{j=1}^{p} \alpha_j . y_{i-j} + \sum_{k=1}^{q} \beta_j \Xi_{i-k} \ , \ \ i = 1, ..., N \tag{2.1}$$

where the dependent random variable is Y_i, x_i is the exogenous variable, the y_i are past values of Y_i and the Ξ_i are unselfcorrelated random variables with zero mean. The regression coefficients α_0, α_j and β_j are estimated from the data and p and q are small positive integers. The notation is intended to make a clear distinction between random variables which are Latin upper case, and constants, such as past values of random variables, which are Latin lower case. Equation (2.1) is a state space representation [4] describing states of the system at a succession of discrete instants; the random variable, Y_i, at one instant becomes the constant, y_i, in the following instant.

The direction of time is important in regression, which, unlike correlation, allows causality to be inferred.

There are software packages for parameter estimation available under the aegis of the major programming languages. Unfortunately some of these are flawed, because they estimate the exogenous parameter, α_0, prior to estimating the other parameters, leading to omitted-variable bias [5]; all parameters must be estimated simultaneously in a regression model.

Estimation of the MA coefficients, $\{\beta_i\}$, requires an iterative Kalman filter method which may not converge. The second, moving average summation in (2.1), describes a convoluting or "blurring" function, so that $q > 1$ when the sampling interval, Δt, is too small. Estimation of the MA coefficients can be avoided by decimating the time series by q to give a new time series with a larger sampling interval, $q\Delta t$, for which the innovation sequence, $\{\Xi_m\}$, is unselfcorrelated. Then (2.1) becomes

$$Y_m = \alpha_0 x_m + \sum_{n=1}^{p} \alpha_n . y_{m-n} + \Xi_m \ , \ \ m = 1, ..., M \tag{2.2}$$

where $m = qi$, $qM \leq N$, The model summarized by (2.2) is an ARX(p) model for 'autoregressive with exogenous variable'. The regression coefficients, α_i, and their confidence limits are estimated using Ordinary Least Squares. The sequence of residuals, $\{\xi_m\}$, is given by

$$\xi_m = y_m - \left(\hat{\alpha}_0 x_m + \sum_{n=1}^{p} \hat{\alpha}_n . y_{m-n} \right) \ , \ \ m = 1, ..., M \tag{2.3}$$

where y_m is the sample value or 'realization' of Y_m and $\hat{\alpha}_0$ to $\hat{\alpha}_p$ are the regression coefficient estimates. The $\{\xi_m\}$ are tested using the Ljung-Box, Q statistic with probability P [6]. The minimum number of coefficients, $\hat{p}$, is found for which P is greater than some confidence level, say 0.1, for which it can be assumed the innovation sequence is not self-correlated.

Our best estimate of the relationship between the two time series is then

$$\sum_{n=0}^{\hat{p}} \hat{\gamma}_n y_{m-n} = \hat{\alpha}_0 x_m \tag{2.4}$$

where

$$\hat{\gamma}_0 = 1 \tag{2.5}$$

$$\hat{\gamma}_n = -\hat{\alpha}_n \ , \ \ n = 1, ..., \hat{p} \tag{2.6}$$

The sequence $\{\gamma_n\}$ specified by (2.4) is the prediction error filter of the autoregressive process.

3. Convolution

We can define a time series more precisely as a finite or semi-infinite sequence, $\{x_0, x_1, x_2, ...\}$ for which the index specifies successive equally spaced intervals of time. The convolution, $c = \{c_k; k = 0, 1, ..., r\} = a * b$, of two time series $a = \{a_i; i = 0, 1, ..., p-1\}$ and $b = \{b_j; j = 0, 1, ..., q\}$, is defined by

$$c_k = \sum_{i+j=k} a_i b_j \tag{3.1}$$

Under this definition convolution satisfies the commutative, associative and distributive laws of arithmetic. Note also that

$$\sum_i a_i \cdot \sum_j b_j = \sum_k \sum_{i+j=k} a_i b_j = \sum_k c_k \tag{3.2}$$

The sum on the left hand side of (2.4) is a convolution and (2.4) can be written

$$\hat{\gamma} * y = \hat{\alpha}_0 x \tag{3.3}$$

A more useful form of (3.3) is

$$y = \hat{I} * x \tag{3.4}$$

where $\hat{I}$ is the convolutional reciprocal of $\hat{\gamma}/\hat{\alpha}_0$ given by

$$\hat{I} * \hat{\gamma} = \hat{\alpha}_0\{1\} \tag{3.5}$$

and will is termed the impulse response. It can be estimated numerically by iteration using (3.5) in the form

$$\hat{I}_m = \sum_{i=1}^{p} \hat{\alpha}_i \hat{I}_{m-i} + \hat{\alpha}_0 \delta_m \tag{3.6}$$

For display purposes and inter-comparison a normalized impulse response, $\Im$, may be used where

$$\Im * \gamma = \{1\} \tag{3.7}$$

Thus the normalized impulse response is the convolutional inverse of the prediction error filter.

Like the regression coefficients, I is a property of the system under investigation and $\hat{I}$ is its estimate. Equation (3.4) describes the output of the system, y, in response to *any* input sequence, x.

The sensitivity of the system, S, is defines as the response at infinity to a unit step function, H_j, where $H_j = 0$ for $j < 0$ and $H_j = 1$ for $j \geq 0$. From (3.1)

$$S = \lim_{k\to\infty} S_k = \lim_{k\to\infty} \sum_{i+j=k} I_i H_j = \sum_{k=0}^{\infty} I_k \tag{3.8}$$

i.e. it is the sum of the terms of the impulse response. It is a random variable on which confidence limits can be placed.

According to (3.2) the sum of a convolution is equal to the product of the sums of the convoluting factors. Thus, from (3.5)

$$\sum_{m=0}^{\infty} I_m \sum_{n=0}^{p} \gamma_n = S \sum_{n=0}^{p} \gamma_n = \alpha_0 \tag{3.9}$$

from which $\hat{S}$ can be estimated in terms of the prediction error filter, $\{\hat{\gamma}_n\}$.

Furthermore, from (2.5), (2.6) and (3.9) any given sensitivity estimate, $\hat{S}$, can be used to define a constraint in the form of a null hypothesis, $\mathcal{H}$, viz.:

$$\mathcal{H} : \hat{\alpha}_0 + \hat{S} \sum_{n=1}^{\hat{p}} \hat{\alpha}_n = \hat{S} \tag{3.10}$$

From (3.10) a distribution of the probability of estimated sensitivity, $\hat{S}$, can be found using the t-test method provided by most Ordinary Least Squares software packages.

4. Global Average Temperature vs ln(CO2)

I estimated the impulse response of the global average temperature anomaly, T, on the logarithm of atmospheric carbon concentration, $\ln(C)$. From this I derived an estimate of sensitivity, $\hat{S}_c$, and its probability distribution.

Global average temperature anomaly data, T. were taken from the `HadCRUT.4.5.0.0` data set [7]. Carbon dioxide concentrations, C, were taken from the University of Melbourne Greenhouse Gas Factsheet [8].

The ARX method was applied to annual means of global average temperature, T_i, on the logarithm of atmospheric CO_2 concentration, $\ln(C_i)$, for the interval 1850 CE to 2014 CE. Applying Ljung-Box to the residuals given by (2.3) for ARX(p), p= 0, ... ,5) gives the results shown in Table 1. The probability, P, for the ARX(4) run has a value of 0.2534 indicating that the null

hypothesis that the residuals are unselfcorrelated cannot be rejected. Thus the simplest regression relationship between T_i, and $\ln(C_i)$ which unambiguously fits the data is the ARX(4) model, viz.:

$$T_i = \hat{\alpha}_0 \ln(C_i) + \hat{\alpha}_1 T_{i-1} + \hat{\alpha}_2 T_{i-2} + \hat{\alpha}_3 T_{i-3} + \hat{\alpha}_4 T_{i-4} \ , \ i = 5, ..., N \tag{4.1}$$

with the regression coefficient estimates $\{1.161, 0.509, -0.063, 0.057, 0.199\}$. The impulse response was estimated using (3.6) and is shown in Figure 1.

The R-matrix tuple corresponding to (3.10) is

$$R = ([1, \hat{S}, ..., \hat{S}], \hat{S}) \tag{4.2}$$

This was used in the t-test method of the *Python statsmodels OLS* software package to determine probability as a function of estimated sensitivity. The results are shown in Figure 2. Note that the sensitivity, S, of (3.9) and (3.10) is the response to a sustained unit change of the independent variable whereas the climate sensitivity, $\hat{S}_c$, plotted in Figure 2 is conventionally defined as the response to a doubling of atmospheric CO_2 concentration. Hence

$$\hat{S}_c = \ln(2)\hat{S} \tag{4.3}$$

From (3.9), (4.1) and (4.3) , estimated global climate sensitivity, $\hat{S}_c = 2.7^{\circ}$C with confidence limits 2.3°C and 3.4°C.

5. CO2 vs Emissions

The response of atmospheric CO2 concentration to an emission pulse in CO2 is discussed extensively by Joos *et al* [9] and, more recently, in the multi-model analysis of Joos *et al* [10]. A mathematical formulation was derived numerically by Meier-Reimer and Hasselmann [11] using a similar model, viz:

$$\Im(t) = A_0 + \sum_{j=1}^{4} A_j \exp(-t/\tau_j) \tag{5.1}$$

where $\Im(t)$ is the normalized impulse response function. The A_j are the proportions corresponding to various decay times, τ_j. $\sum A_j = 1$ and, importantly, $A_0 = .131$. The time constants range from 362.9 years to 1.9 years. Equation (5.1) is plotted as the dashed line in Figure 3. The curve is typical of the IRF curves quoted by Joos *et al*.

For comparison, the ARX method developed here was applied to annual means of atmospheric CO_2 concentration [8], C_i, vs global fossil fuel emissions, E_i. Global fossil fuel emissions, E, for the interval 1850 to 2014, were downloaded from the Carbon Dioxide Information Analysis Center [12].

Applying the Ljung-Box test to the residuals given by (2.3) for ARX(p), p= 0, ... ,5) resulted in zero probabilities in all cases. The ARMAX method revealed a significant moving average component with $q = 2$. For this reason both time series were decimated by 2 and the ARX / Ljung-Box method reapplied. The results for the decimated data are shown in Table 2. The probability, P, for the ARX(1) run has a value of 0.4359 indicating that the null hypothesis that the residuals are unselfcorrelated cannot be rejected. Thus the simplest regression relationship between C_i and E_i which unambiguously fits the data is the ARX(1) model, viz.:

$$C_i = \hat{\alpha}_0 E_i + \hat{\alpha}_1 C_{i-1} \ , \ i = 1, ..., N \tag{5.2}$$

where the estimated regression coefficients are $\hat{\alpha}_0 = 0.21$ and $\hat{\alpha}_1 = 0.969$ with 95 percent confidence limits 0.945 and 0.992. The prediction error filter is $\{1, -\hat{\alpha}_1\}$ which has convolutional inverse $\{1, \hat{\alpha}_1, \hat{\alpha}_1^2, ...\}$, a geometric sequence with common ratio $\hat{\alpha}_1$. The nth term of the IRS

estimate is given by

$$\hat{I}_n = \hat{\alpha}_0 \hat{\alpha}_1^n = \hat{\alpha}_0 \exp(-\frac{nq\Delta t}{\tau}) \tag{5.3}$$

and the impulse response can be regarded as discretely sampled from a continuous exponential function with time constant given by

$$\tau = -q\Delta t / \ln(\hat{\alpha}_1) \tag{5.4}$$

Substituting $\hat{\alpha}_1$ and its confidence limits into (5.4) and multiplying by ln(2) gives a half-time of 43 years with confidence limits of 24 years and 193 years. The normalized impulse response is shown in Figure 3.

The R-matrix tuple corresponding to (3.10) is

$$R = ([1, \hat{S}], \hat{S}) \tag{5.5}$$

This was used in the t-test method of the *Python statsmodels OLS* software package to determine probability as a function of estimated sensitivity. The results are shown in Figure 4.

6. Local Temperature vs ln(CO2)

A netCDF dataset of local mean monthly temperatures for the entire globe was downloaded [13]. Each temperature value was associated with a 5 degree latitude by 5 degree longitude spherical rectangle, there being 36 X 72 such rectangles. Time series of annual averages were computed for each rectangle for comparison with the above described time series of $\ln(C_i)$ using the ARX(p) method. The Ljung-Box P value was found for candidate values of p in the range $0 < p \leq 5$. The smallest value of p for which

$$P > 0.1 \tag{6.1}$$

was chosen as the order of the ARX process and (3.9) solved for S.

Spherical rectangles were eliminated from further processing when the number of years of good data was less than fifty or when no value of P satisfying (6.1) could be found. In a surprising number of cases p was zero in which case S was simply the first order regression coefficient of temperature on concentration.

Local sensitivity estimates are mapped in Figure 5. For ease of display S values were rounded to the nearest integer.

7. Discussion

The climate sensitivity estimate and its confidence limits shown in Figure 2 are not dissimilar from values proposed by the IPCC. On the other hand, the impulse response and sensitivity of CO_2 concentration estimated here are quite different from conventionally accepted values. The impulse response has an exponential decay with a single time constant (Figure 3) and the sensitivity estimate is finite (Figure 4). These statistics were derived from an ARX regression model which was an excellent fit to the observations with no self-correlation evident in the residuals (Table 2).

The impulse response function (5.1) due to Meier-Reimer and Hasselmann [11] must be integrated from zero to infinity with respect to time in order to give the sensitivity. Their sensitivity is therefore infinite because of the non-zero term, A_0, in (5.1) according to which thirteen percent of CO_2 emissions remains in the atmosphere indefinitely. In contrast the sensitivity estimated here from observations is finite with finite 95 percent confidence limits. This reveals a serious shortcoming of their dynamical global ocean circulation model.

A possible explanation is the following. The deep ocean is bounded by a turbulent mixed layer and by the highly turbulent Antarctic Circumpolar Current. It is therefore likely to be internally mixed by a Kolmogorov cascade of turbulent eddies, some with spatial scales as large as ocean basins and with time scales of, perhaps, decades. Turbulence is a stochastic phenomenon which

is difficult to observe at large spatial and temporal scales and which, being stochastic, cannot be readily emulated by deterministic models such as OAGCMs. Eddy diffusion generated by turbulent mixing would greatly increase the capacity of the deep ocean to absorb carbon dioxide and so could account for the shorter half time of the observed impulse response of atmospheric CO_2 concentration. Whatever the explanation, there is no evidence for the long half times and remnant component of atmospheric CO_2 concentration in (5.1), presently assumed by most modellers.

The map of local sensitivities (Fig 5) demonstrates the viability of the present method. Extreme values tend to lie close together: for example the occurrence of zero values in the North Atlantic and the occurrence of larger values over land. If the method were only generating noise, we would not expect such good spatial correlation. High values of S_c in Northern Canada and Siberia suggest that, in these locations, CO_2 concentration is the predominant factor controlling nocturnal radiative cooling in the absence of clouds. No explanation can be offered for the low values in the North Atlantic except that perhaps other factors, such as submarine volcanism, may play a role in modulating Sea Surface Temperature there. Two unusually high maritime values of $S_c = 4°\mathrm{C}$ off the SE corner of Australia near the island of Tasmania may be due to the intermittent incursion of the warm East Australia Current into this region.

Figure 5 is only the first, tantalizing glimpse of the possibilities presented by applying rigorous statistical methods to climate change. The effect of CO_2 concentration on other types of observations, such as precipitation, wind speed and so on, remain to be explored. The strong spatial gradients in climate sensitivity observed in places such as Southern California, imply that mean temperature *gradients* are affected by climate change and this too has meteorological implications.

Statistical methods provide fresh insights into the underlying physics of climate change, insights that are not accessible to numerical general circulation models.

References

1. Tang W, Llort J, Weis J, Perron MMG, Basart S, Li Z, et al.
   Widespread phytoplankton blooms triggered by 2019-2020 Australian wildfire.
   Nature. 2021;597:370–389.
2. Box GEP, Jenkins G.
   Time Series Analysis: Forecasting and Control.
   San Francisco, CA: Holden-Day; 1976.
3. Mills TC.
   Applied Time Series Analysis: A Practical Guide to Modelling and Forecasting.
   Cambridge, Mass: Academic Press; 2019.
4. Hamilton EJ.
   Time Series Analysis.
   Princeton, New Jersey: Princeton University Press; 1994.
5. Greene WH.
   Econometric Analysis (5th ed.).
   New Jersey: Prentice Hall; 2003.
6. Ljung GM, Box GEP.
   On a Measure of a Lack of Fit in Time Series Models.
   Biometrika. 1978;65:297–303.
7. Morice CP, Kennedy JJ, Rayner NA, Winn JP, Hogan E, Killick RE, et al.
   An updated assessment of near-surface temperature change from 1850: the HadCRUT5 dataset.
   Journal of Geophysical Research: Atmospheres 2021;126(3):e2019JD032361
   Available from: https://www.uea.ac.uk/documents/96135/5574306/CRU-Info-sheet-2021.pdf/ef760d3e-a3ee-cebd-e0df-9ae1a3020162?t=1629562617072.
8. Meinshausen M, Vogel E, Nauels A, Lorbacher K, Meinshausen N, Etheridge DM, et al.
   Historical greenhouse gas concentrations for climate modelling (CMIP6).
   Geosci Model Dev. 2017;10:2057–2116.

9. Joos F, Bruno M, Fink R, Siegenthaler U, Stocker TF, Le Quere C, et al.
An efficient and accurate representation of complex oceanic and biospheric models of anthropogenic carbon uptake.
Tellus B: Chemical and Physical Meteorology. 1994;48(3):394–417.
10. Joos F, Roth R, Fuglestvedt JS, Peters GP, Enting IG, von Bloh W, et al.
Carbon dioxide and climate impulse response functions for the computation of greenhouse gas metrics: a multi-model analysis.
Atmospheric Chemistry and Physics. 2013;13(5):2793–2825.
Available from: https://acp.copernicus.org/articles/13/2793/2013/.
11. Maier-Reimer E, Hasselmann K.
Transport and storage of CO2 in the ocean - an inorganic ocean-circulation carbon cycle model.
Climate Dynamics. 1987;2:63–90.
Available from: https://doi.org/10.1007/BF01054491.
12. Boden TA, Marland G, Andres RJ.
Global, Regional, and National Fossil-Fuel CO2 Emissions.
Carbon Dioxide Information Analysis Center, Oak Ridge National Laboratory, US Department of Energy, Oak Ridge, Tenn, USA. 2017;.
Available from: https://cdiac.ess-dive.lbl.gov/ftp/ndp030/global.1751_2014.ems.
13. Morice CP, Kennedy JJ, Rayner NA, Winn JP, Hogan E R E Killick et al.
An updated assessment of near-surface temperature change from 1850: the HadCRUT5 data set.
Journal of Geophysical Research: Atmospheres. 2021;126:e2019JD032361.
Available from: https://www.metoffice.gov.uk/hadobs/hadcrut5/data/current/download.html.

Table 1. Ljung-Box parameter, Q, and its probability, P, for five ARX runs of global average temperature vs. the logarithm of CO_2 concentration.

Run	Variables	Q	P
ARX(0)	T_i vs ln(C_i) only	284.1	0.0000
ARX(1)	T_i vs ln(C_i), T_{i-1}	49.0	0.0084
ARX(2)	T_i vs ln(C_i),T_{i-1},T_{i-2}	48.2	0.0074
ARX(3)	T_i vs ln(C_i),T_{i-1} to T_{i-3}	40.4	0.0358
ARX(4)	T_i vs ln(C_i),T_{i-1} to T_{i-4}	29.3	0.2534
ARX(5)	T_i vs ln(C_i),T_{i-1} to T_{i-5}	28.6	0.2367

Table 2. Ljung-Box parameter, Q, and its probability, P, for five ARX runs of CO_2 concentration, C, vs. global fossil fuel emissions, E. Both time series were decimated by 2.

Run	Q	pvalue
C(t) vs E(t) only	513.5	0.0000
C(t) vs E(t), C(t-1)	28.5	0.4359
C(t) vs E(t),C(t-1),C(t-2)	28.6	0.3830
C(t) vs E(t) to C(t-3)	24.5	0.5483
C(t) vs E(t) to C(t-4))	24.3	0.5049
C(t) vs E(t) to C(t-5)	22.0	0.5796

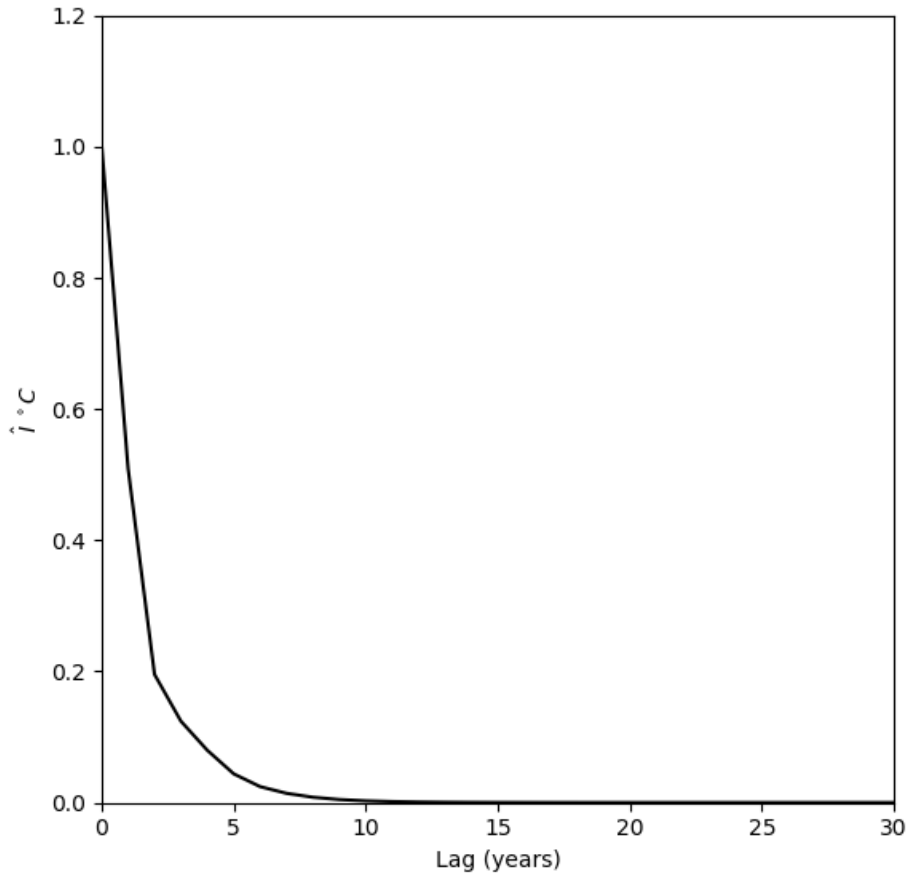

Figure 1. The normalized impulse response, $\Im$, of Global Average Temperature due to an impulse in Carbon Dioxide Concentration.

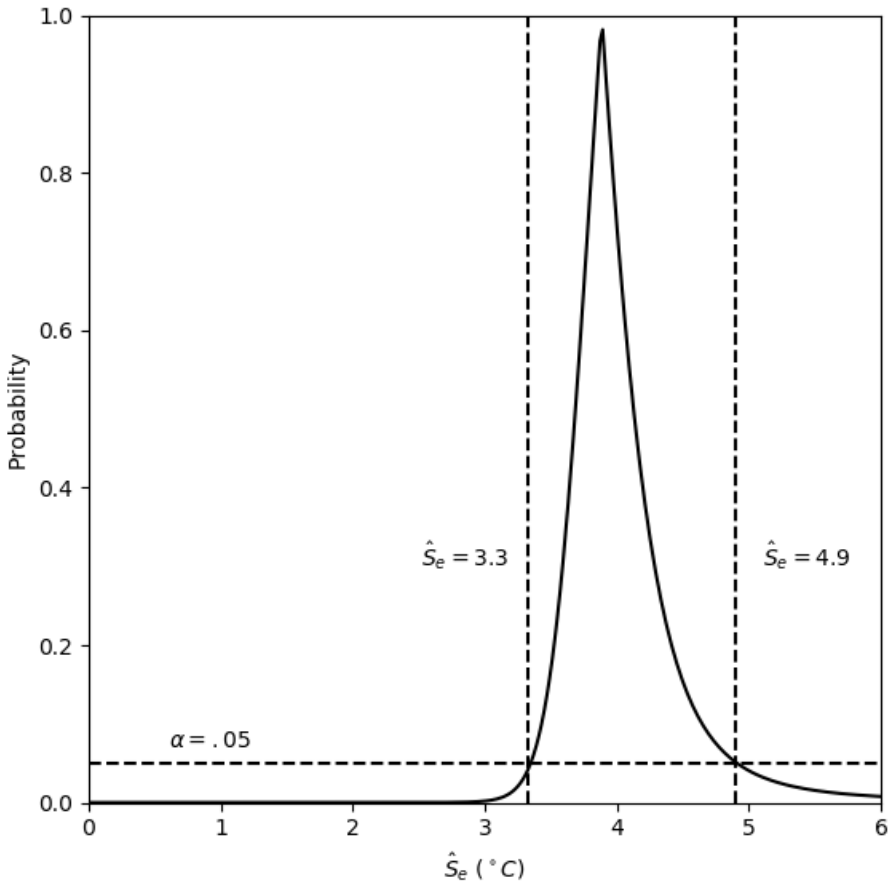

Figure 2. The t-test probablity, P, that the sensitivity, S, of global average temperature will have a given value. The peak is at $S = 3.9°$C. The vertical dashed lines are the 95 percent confidence limits, (3.3°C and 4.9°C). Climate Sensitivity is therefore $S_c = 2.7°$C with confidence limits 2.3°C and 3.4°C.

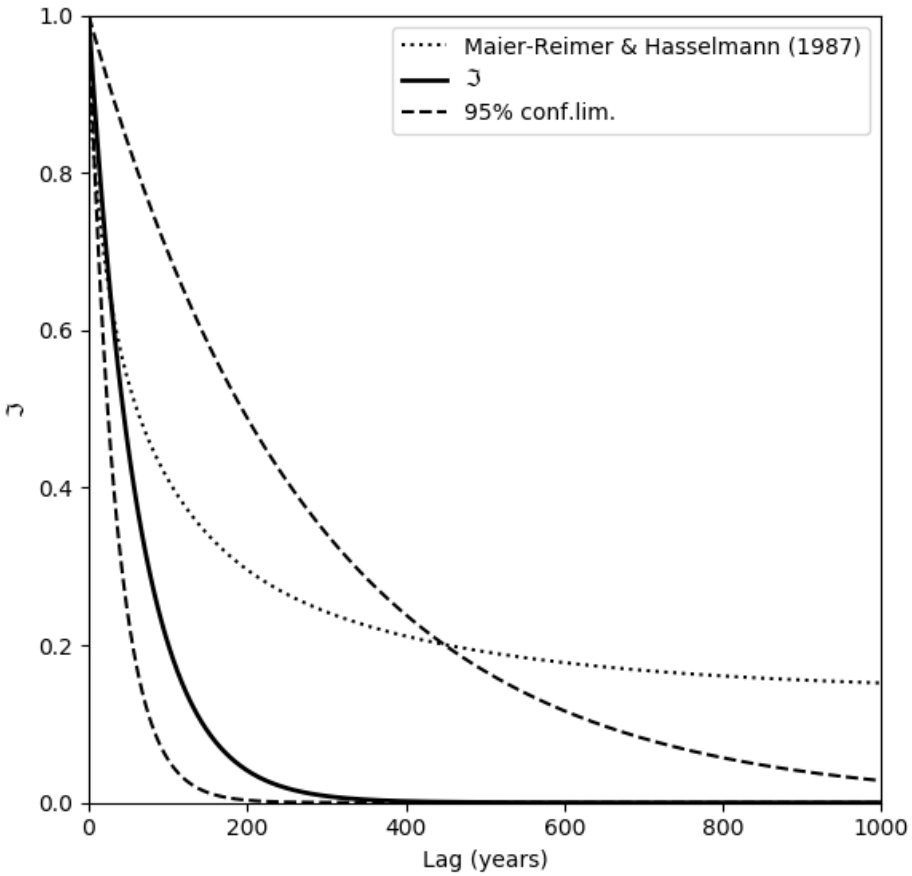

Figure 3. The observed normalized impulse response, $\Im$, of Carbon Dioxide concentration due to an impulse in CO2 emissions (solid line) with its 95% confidence limits (dashed lines). Also shown is the model-derived normalized impulse response function of Meier-Reimer and Hasselmann [11] (dotteded line).

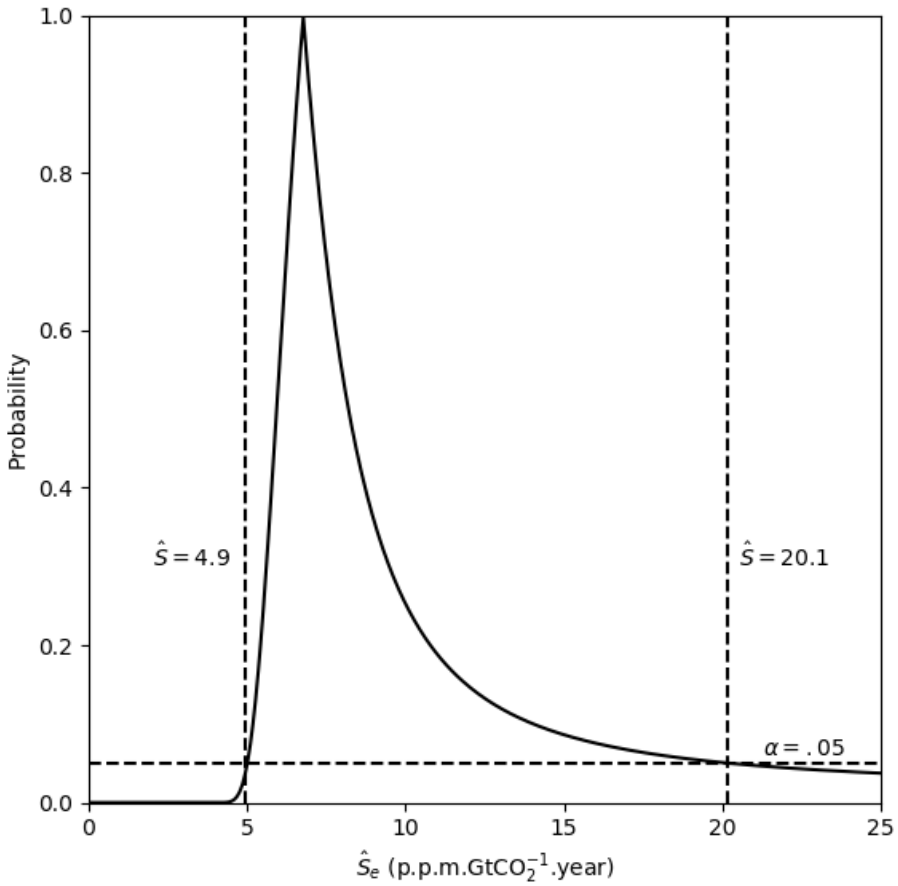

Figure 4. The t-test probablity, P, that the sensitivity, S, of CO_2 concentration will have a given value. The peak is at $S = 6.77$ p.p.m.GtCO$_2^{-1}$.year. The vertical dashed lines are the 95 percent confidence limits.

.

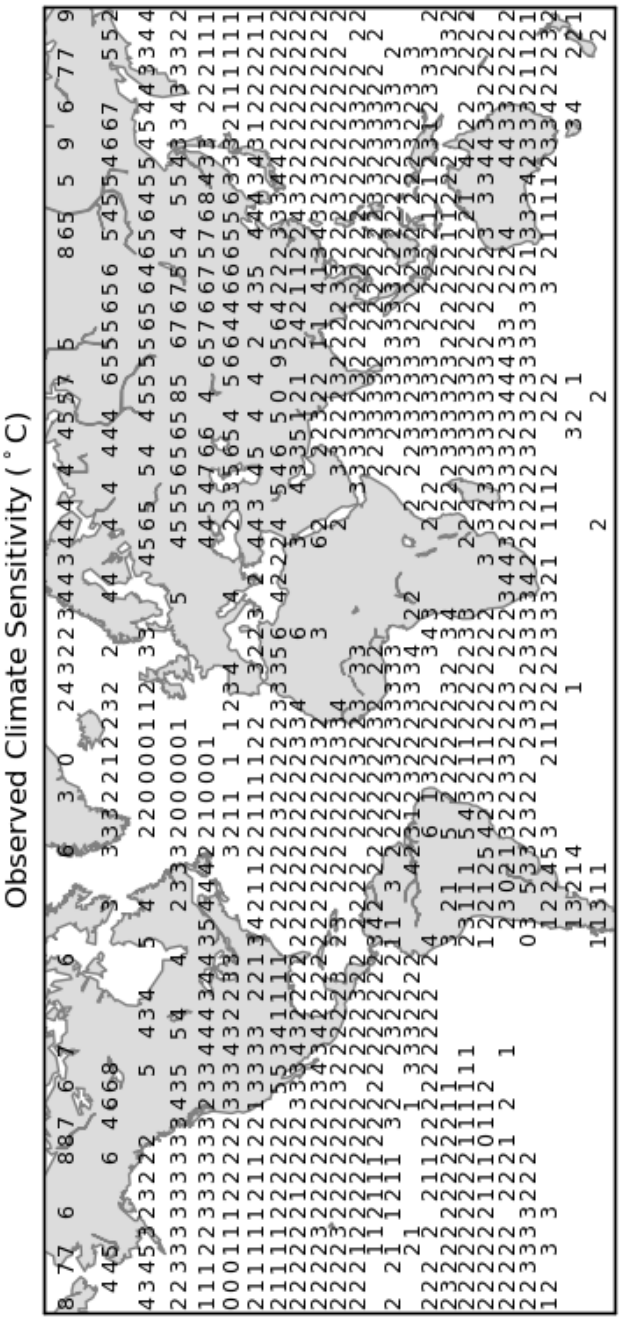

Figure 5. Figure Caption: Climate Sensitivity, S_c estimated for 5 deg X 5 deg rectangles of the earth's surface. Each estimate is derived from the time series of annual average surface air temperature of the rectangle using the ARX method with the time series of ln(CO2 concentration) as the exogenous variable. Only those estimates from rectangles with more than 50 data points and unselfcorrelated residuals are shown. Displayed values have been rounded to the nearest integer.